Advanced Robotics

ISSN: 0169-1864 (Print) 1568-5535 (Online) Journal homepage: http://www.tandfonline.com/loi/tadr20

Online Balance Controllers for a Hopping and Running Humanoid Robot

Baek-Kyu Cho , Jung-Hoon Kim & Jun-Ho Oh

To cite this article: Baek-Kyu Cho , Jung-Hoon Kim & Jun-Ho Oh (2011) Online Balance Controllers for a Hopping and Running Humanoid Robot, Advanced Robotics, 25:9-10, 1209-1225, DOI: 10.1163/016918611X574687

To link to this article: https://doi.org/10.1163/016918611X574687

Published online: 02 Apr 2012.

///VSP///
Advanced Robotics 25 (2011) 1209–1225
ADVANCED ROBOTICS
brill.nl/ar

Full paper

Online Balance Controllers for a Hopping and Running Humanoid Robot

Baek-Kyu Cho [a,b], Jung-Hoon Kim [b,*] and Jun-Ho Oh [c]

[a] Robotics Institute, Carnegie Mellon University, 5000 Forbes Avenue, Pittsburgh, PA 15213, USA
[b] Construction Robot and Automation Laboratory, Department of Civil and Environmental Engineering, Yonsei University 134 Shinchon-dong, Seodaemun-gu, Seoul 120-749, South Korea
[c] Hubo-Lab, Department of Mechanical Engineering, KAIST, 335 Gwahangno, Yeseong-gu, Daejeon 307-701, South Korea

Received 17 February 2010; accepted 12 May 2010

Abstract

This paper describes online balance controllers for running in a humanoid robot and verifies the validity of the proposed controllers *via* experiments. To realize running in the humanoid robot, the overall control structure is composed of an offline controller and an online controller. The main purpose of the online controller is to maintain dynamic stability while the humanoid robot hops or runs. The online controller is composed of the posture balance control in the sagittal plane, the transient balance control in the frontal plane and the swing ankle pitch compensator in the sagittal plane. The posture balance controller makes the robot maintain balance using an inertial measurement unit sensor in the sagittal plane. The transient balance controller makes the robot keep its balance in the frontal plane using gyros attached to each upper leg. The swing ankle pitch compensator prevents the swing foot from hitting the ground at unexpected times while the robot runs forward. HUBO2 was used for the running experiment. It was designed for the running experiment, and is lighter and more powerful than the previous walking robot platform, HUBO. With the proposed controllers, HUBO2 ran forward stably at a maximum speed of 3.24 km/h and this result verified the effectiveness of the proposed algorithm. In addition, in order to show the contribution of the stability, the running performance according to the existence of each controller was described by experiment.

Keywords

Humanoid, running, biped robot, HUBO2, balance

1. Introduction

The appearance of new humanoid robots is no longer a surprise. Various humanoid robots are announced every year through exhibitions, the internet, TV and so on.

* To whom correspondence should be addressed. E-mail: junghoon@yonsei.ac.kr

 DOI:10.1163/016918611X574687

One of the ultimate purposes of these robots is to help human beings. With intelligent abilities such as manipulation, mobility, navigation, recognition and human–robot interaction, humanoid robots will provide services to human beings at home or work, improving the quality of life. For example, Honda's ASIMO has given many demonstrations of delivering beverages to people on a tray, helping elderly people and so on (http://world.honda.com/ASIMO). In addition, HUBO [1] and HRP-2 [2] have given similar demonstrations. HRP-2 has also given demonstrations of teleoperation of a remote excavator at a construction site and cooperation with humans in installing panels. However, if the safety of the robot is not guaranteed, the robot cannot help people, but may cause harm to them. Therefore, a controller that guarantees stability can be regarded as the most important issue in the real application of robots in our daily lives.

Locomotion is classified into walking and running. Even though running is more unstable than walking, the fast mobility of running is very attractive. For this reason, the study of running is ongoing in many places. The pacesetters of humanoid running are Honda's ASIMO [3, 4] and Toyota's Partner robot [5]. According to an announcement in 2005, the newest version of ASIMO can walk at a maximum rate of 2.7 km/h and can run at a maximum rate of 6 km/h. In addition, the Partner robot can run at a maximum rate of 7 km/h, which is faster than ASIMO. In addition, Sony's QRIO [6], AIST's HRP-2LR [7] and others are being used in further research into running. However, the running algorithms of ASIMO and the Partner robot have not been announced in public, and the other robots, except for ASIMO and the Partner robot, do not show strong running ability. Also, Chevallereau *et al.* tried to realize running with the planar robot, but it ran only six steps [8]. Even though it is not a humanoid robot, Raibert realized running with 3D Biped [9].

Therefore, this paper describes an online controller to raise the stability when a humanoid robot hops or runs. The validity of the controller is verified by experiment using HUBO2. This robot was developed at KAIST in 2008. Since it is lighter and more powerful than HUBO, it is suitable for use in research on running. The running pattern of HUBO2 is generated offline by the running pattern generation method, which has been studied in previous research [10]. The running pattern is generated with the Poincare map of single-step running and its fixed point to make a natural and periodic running pattern. The fixed point is calculated numerically. In addition, an online controller for running is applied to HUBO2 in real-time to realize stable running.

This paper is organized as follows. In Section 2, the humanoid robot used in this paper, HUBO2, is explained. In Section 3, the online controller for running in humanoid robots is explained. The online controller is composed of three controllers: (i) the posture balance controller in the sagittal plane makes the humanoid robot maintain its balance and reduces the vibration in the sagittal plane, (ii) the transient balance control in the frontal plane prevents the humanoid robot from falling in the frontal plane and (iii) the swing ankle pitch compensator in the sagittal plane keeps the swing foot of the humanoid robot from touching the ground while the humanoid robot runs. In Section 4, the controllers are verified in experiments. Finally, Section 5 concludes the paper.

2. Overview of the Humanoid Robot HUBO2

HUBO2, developed in 2008, is shown in Fig. 1. It has a total of 40 d.o.f., including 12 d.o.f. in the lower limbs, 1 d.o.f. in the waist, 14 d.o.f. in the two arms, 10 d.o.f. in the two hands and 3 d.o.f. in the neck. In the development of HUBO2, the design objective was focused on a reduction in weight and an increase in actuator power. Therefore, HUBO2 is more suitable than HUBO for running research. The total weight of HUBO2, including the battery, exterior case, computer, sensors, controllers and amplifiers, is 45 kg. This is only 69% of the weight of HUBO, which weighed 65 kg. To reduce the weight and produce the high power, the CSF-type harmonic drive gear and 150 W DC motor used in HUBO were replaced with an SHD-type harmonic drive gear and 200 W BLDC motor. Also, synthetic resins are attached at the four corners of both soles to protect the robot from the landing impact. See Table 1.

HUBO2 uses a distributed control system — the main computer managing the overall operation of the robot and the joint motor controllers (JMCs) controlling

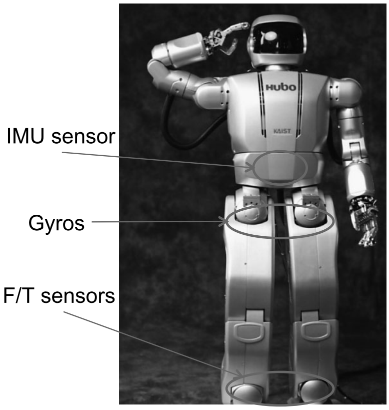

Figure 1. HUBO2.

Table 1.
HUBO *versus* HUBO2

	HUBO	HUBO2
Total weight (kg)	65	45
Weight of major motor (kg)	0.447 (150 W DC motor)	0.283 (200 W BLDC motor)
Weight of major harmonic drive (kg)	0.947	0.511

the motor of the robot are connected through controller area network (CAN) communication. If the main computer sends position commands to the JMC, each JMC control assigns the motor to move to the commanded position. Some sensory devices attached on the robot are used for posture control and motion control, and these communicate with the main computer through the CAN. Since the main computer is attached inside the humanoid robot, a wireless local area network (LAN) is used to access the main computer.

In HUBO, the main computer and the JMCs communicate every 10 ms by the CAN. In order to realize running, 100 Hz of control loop is not sufficient. Therefore, in HUBO2, the lower body of the robot and the sensory devices that mainly affect stability communicate every 5 ms with the main computer, while the upper body and the head of the robot communicate every 10 ms with the main computer.

In this study, an inertia measurement unit (IMU), a gyro and force/torque (F/T) sensors are used. An IMU sensor is attached to the upper body of the robot, and measures the angles and angular velocities against the ground in the sagittal and frontal planes. The IMU sensor is composed of an inclinometer and a gyro. Other gyro sensors are used to measure the angular velocity of the stance leg in the frontal plane; these sensors are attached to both thighs, as shown in Fig. 1. Also, F/T sensors are attached at the ankle joints, and measure the normal force in the vertical direction and two moments along the roll and pitch axes. They are used to detect the landing and flying timings.

3. Online Controllers for Running

To realize locomotion of a humanoid robot, an offline controller and an online controller are required. The offline controller calculates such things as walking or running patterns, and the online controller works based in real-time on sensor feedback when the robot moves. The running pattern included in the offline controller was dealt with in the previous research [8] and the online controller, which produces a stable balance when the robot hops or runs, is described in this paper.

The control structure of HUBO2 used in this research is shown in Fig. 2. The left part is the offline controller. According to the desired running velocity, all of the joint trajectories are obtained by the offline controller, which is the running pattern generator. On the other hand, the right part is the online controller, which enables the humanoid robot to maintain balance in real-time.

The online controller of the HUBO2 used in this research is composed of two control loops, as shown in Fig. 2. The first control loop is concerned with the position control of the motor and it works every 1 ms inside of the JMC. A general PD feedback controller is used here. The second control loop includes the online controller for running; this one works every 5 ms, which is the same as the timer interrupt of the main computer. The main computer generates the position command for each joint motor by adding the reference angles of the offline running pattern generator with the results of the online controllers. Then, the computer sends the motor command to the JMCs *via* the CAN. These are the important roles of the

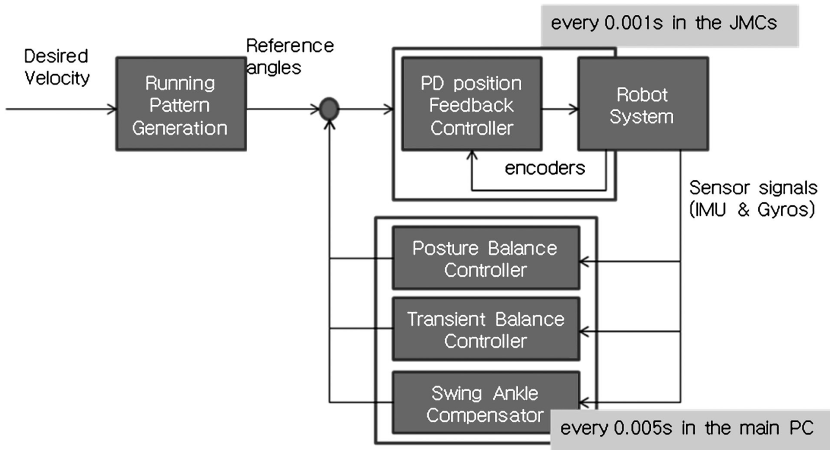

Figure 2. Structure of control system.

main computer. The online controller for running is composed of three controllers, which are the posture balance controller in the sagittal plane, the transient balance controller in the frontal plane and the swing ankle compensator in the sagittal plane. Since running is a larger and faster movement than walking, instability of the robot can be easily caused. Thus, it is very important to maintain stability. In our algorithm, the balance is basically kept by the posture balance controller in the sagittal plane and the transient balance controller in the frontal plane. With the increase in velocity, the robot can fluctuate back and forth rather than left and right. At such times, the swing foot of the robot can touch the ground at an unexpected time and increase the instability. To prevent this phenomenon, the swing ankle compensator is added in the sagittal plane.

3.1. Posture Balance Controller in the Sagittal Plane

The humanoid robot has a compliant effect due to the geometrical structure of the humanoid robot, reducer, synthetic resins of the sole, compliant F/T sensor and harmonic drive gear. This compliant effect produces a vibration when the robot stands on the ground and the vibration causes instability. Therefore, a posture balance controller in the sagittal plane is proposed to reduce the vibration and keep the balance. This controller is applied only in the sagittal plane. The controller allows the robot to maintain its posture.

3.1.1. System Identification

To design the posture balance controller in the sagittal plane, the humanoid robot in the sagittal plane is simplified, as shown in the model in Fig. 3. Here, m is the total mass of the robot, u is the position command of the motor, g is gravity and L is the distance from the ankle joint to the center of mass. Also, the compliance of the robot is composed of a spring (K) and a damper (C). θ is the real angle of the

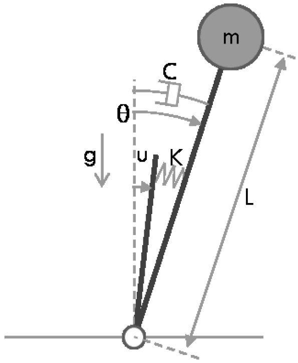

Figure 3. Simple model in the sagittal plane.

robot against gravity, which is measured by the IMU sensor attached at the upper body.

The dynamic equation of the simple model is:

$$mL^2\ddot{\theta} = -C\dot{\theta} - K(\theta - u) + mgL\sin\theta. \tag{1}$$

Equation (1) is linearized as:

$$mL^2\ddot{\theta} + C\dot{\theta} + K\theta - mgL\theta = Ku. \tag{2}$$

The transfer function between θ and u is:

$$\begin{aligned} TF \equiv G(s) = \frac{\Theta(s)}{U(s)} &= \frac{K}{mL^2s^2 + Cs + (K - mgL)} \\ &= \frac{K/(mL^2)}{s^2 + C/(mL^2)s + (K - mgL)/(mL^2)} = \frac{K/(mL^2)}{s^2 + 2\varsigma\omega_n s + \omega_n^2}. \end{aligned} \tag{3}$$

The unknown values of the transfer function are K and C. They are calculated through the analysis of the free vibration response of the robot. The vibration frequency (f_d) and the real number (σ) of pole of the free vibration response are easily estimated. With f_d and σ, the undamped natural frequency (ω_n) and the damping ratio (ς) are calculated as:

$$\begin{gathered} \sigma = \varsigma\omega_n \\ f_d = \frac{\omega_d}{2\pi} \\ \omega_d = \omega_n\sqrt{1-\varsigma^2} = \sqrt{\omega_n^2 - \sigma^2} \\ \therefore \omega_n = \sqrt{\omega_d^2 + \sigma^2} = \sqrt{(2\pi f_d)^2 + \sigma^2} \quad \text{and} \quad \varsigma = \frac{\sigma}{\omega_n}. \end{gathered} \tag{4}$$

Therefore, K and C are calculated as:

$$K = mL^2\omega_n^2 + mgL = mL^2\big((2\pi f_d)^2 + \sigma^2\big) + mgL \tag{5}$$

$$C = 2\varsigma\omega_n mL^2 = 2\frac{\sigma}{\omega_n}\omega_n mL^2 = 2\sigma mL^2. \tag{6}$$

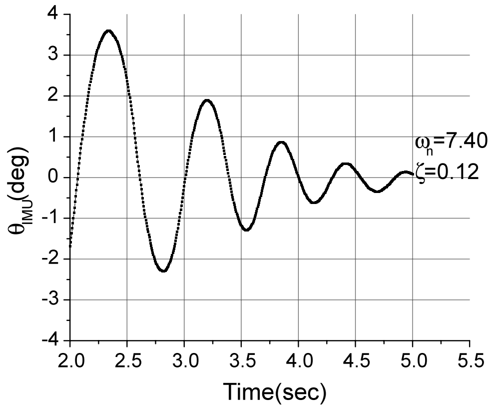

Figure 4. Free vibration response in the sagittal plane.

Figure 4 shows the free vibration response of HUBO2 in the sagittal plane. Therefore, f_d and σ were estimated as:

$$\sigma \approx 0.9$$
$$f_\mathrm{d} \approx 1.17\ \mathrm{Hz}.$$

With (4), ω_n and ς were calculated:

$$\omega_\mathrm{n} \approx 7.4\ \mathrm{rad/s}$$
$$\varsigma \approx 0.12.$$

With (5) and (6), K and C were calculated:

$$K \approx 753\ \mathrm{Nm/rad}$$
$$C \approx 18\ \mathrm{Nm/(rad/s)}.$$

Therefore, the transfer function TF for a simple model of HUBO2 is:

$$TF \equiv G(s) \approx \frac{75.3}{s^2 + 1.8s + 54.9}. \tag{7}$$

3.1.2. Design of the Posture Balance Controller in the Sagittal Plane

The control law is:

$$\begin{aligned} u_{\mathrm{AnklePitch}} &= \theta^{\mathrm{Ref}}_{\mathrm{AnklePitch}} + \theta^{\mathrm{Control}}_{\mathrm{AnklePitch}} \\ &= \theta^{\mathrm{Ref}}_{\mathrm{AnklePitch}} + C_{\mathrm{Filter}} K_{\mathrm{P}}\left(\theta^{\mathrm{Ref}}_{\mathrm{AnklePitch}} - \theta^{\mathrm{IMU}}_{\mathrm{AnklePitch}}\right), \end{aligned} \tag{8}$$

where $\theta^{\mathrm{Ref}}_{\mathrm{AnklePitch}}$ is the prescheduled ankle trajectory in the running pattern generation and $\theta^{\mathrm{Control}}_{\mathrm{AnklePitch}}$ is the control input created by the posture balance controller. The posture balance controller uses a P-controller. The structure of the posture balance controller in the sagittal plane is shown in Fig. 5.

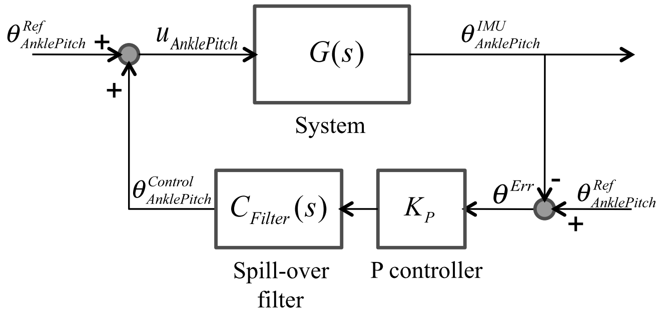

Figure 5. Block diagram of the posture balance controller in the sagittal plane.

The transfer function of the simple model applied the posture balance controller is:

$$
\begin{aligned}
U &= R + C_{\text{Filter}} K_{\text{P}} E \\
E &= R - \Theta \\
\Theta &= GU = G(R + C_{\text{Filter}} K_{\text{P}}(R - \Theta)) \\
(1 + C_{\text{Filter}} K_{\text{P}} G)\Theta &= (G + C_{\text{Filter}} K_{\text{P}} G) R \\
\therefore \frac{\Theta(s)}{R(s)} &= \frac{G + C_{\text{Filter}} K_{\text{P}} G}{1 + C_{\text{Filter}} K_{\text{P}} G},
\end{aligned}
\tag{9}
$$

where U, R, E and Θ indicate the Laplace transforms of $u_{\text{AnklePitch}}$, $\theta^{\text{Ref}}_{\text{AnklePitch}}$, θ^{Err} and $\theta^{\text{IMU}}_{\text{AnklePitch}}$. G is the transfer function of the simple model and K_{P} is the gain of the posture balance controller. C_{Filter} is the transfer function of the spill-over filter. The spill-over filter prevents the unpredicted response caused by the difference between the real humanoid robot and the simple model. K_{P} is calculated by the root locus design method.

According to this procedure, the posture balance controller in the sagittal plane of HUBO2 is designed. The characteristic equation of the system applied controller is:

$$1 + K_{\text{P}} C_{\text{Filter}} G(s) = 0, \tag{10}$$

where:

$$C_{\text{Filter}}(s) = \frac{10}{s + 10} \tag{11}$$

$$G(s) = \frac{75.3}{s^2 + 1.8s + 54.9}. \tag{12}$$

The root locus of the characteristic equation (10) is shown in Figs 6 and 7. Figure 6 shows the root locus when K_{P} is larger than zero (negative feedback) and Fig. 7 shows the root locus when K_{P} is smaller than zero (positive feedback). If K_{P} is set to a positive value, the system diverges. Therefore, K_{P} is set to a negative value.

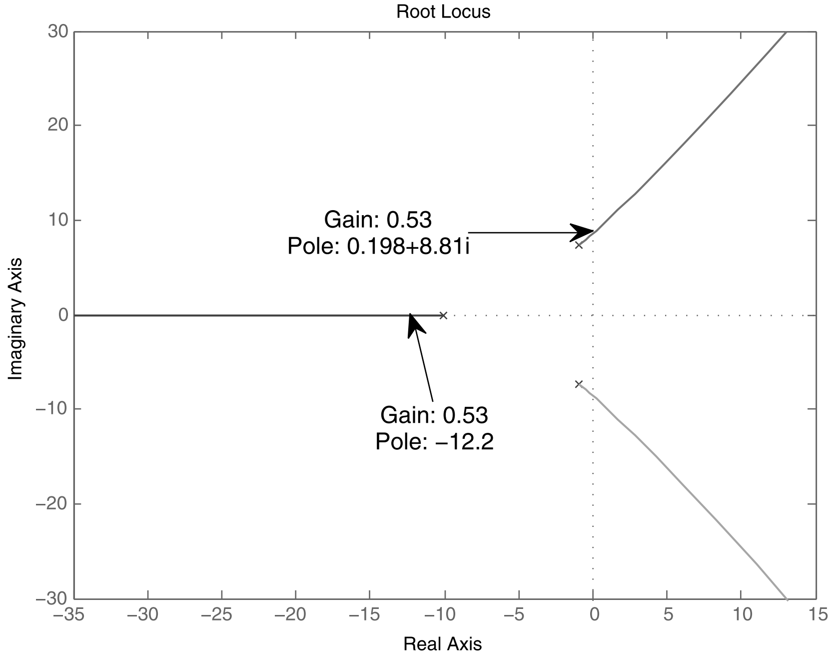

Figure 6. Root locus of negative feedback.

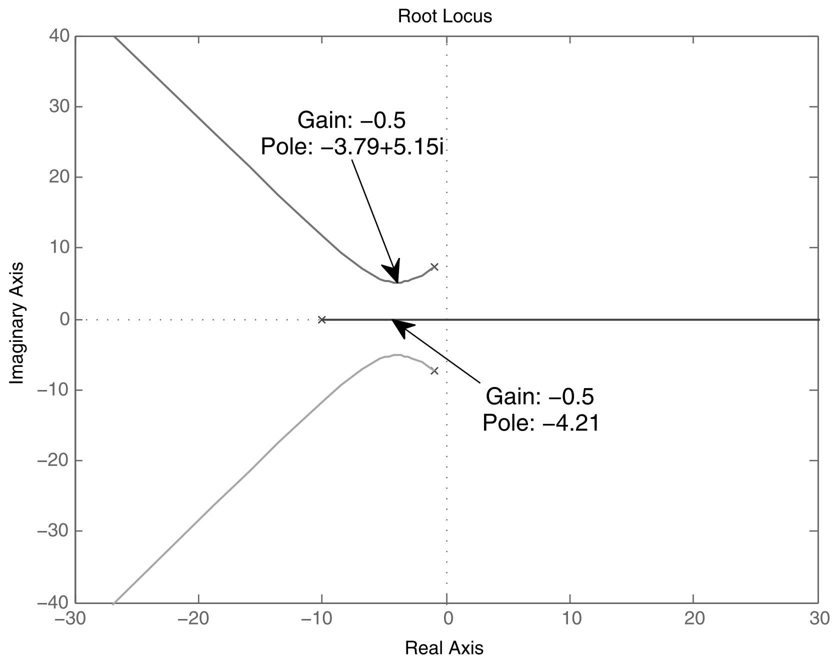

Figure 7. Root locus of positive feedback.

K_P is set to -0.5 in this research. When K_P is -0.5, the damping ratio (ς) becomes 0.59. It is 4.9-times larger than the damping ratio when the posture balance controller is not applied. Since K_P is a negative value, the posture balance controller is the positive feedback controller.

3.2. Transient Balance Controller in the Frontal Plane

In the previous section, the IMU sensor attached at the upper body was used for the posture balance control. However, because the mechanical structure in the frontal plane is a cantilever beam structure, the upper body vibrates largely rather than the stance leg after landing. Therefore, the IMU sensor is not proper for balancing in the frontal plane. To solve this, gyros attached at both thighs are used to produce stability in the frontal plane.

A simple model of the humanoid robot in the frontal plane is shown in Fig. 8. When the robot stands on a single leg, it is assumed to be a single mass inverted pendulum, the same as the simple model in the sagittal plane. Rate gyros attached to both thigh parts measure the inclination rate of the stance leg. When the robot stands on its right leg, the rate gyro attached to the right thigh is used. When the robot stands on its left leg, the rate gyro attached to the left thigh is used. $\theta_{\mathrm{AnkleRoll}}^{\mathrm{Ref}}$ is the prescheduled ankle roll trajectory in the running pattern generation, $\dot{\theta}_{\mathrm{AnkleRoll}}^{\mathrm{Gyro}}$ is the angular velocity of the stance leg measured by the rate gyro and $u_{\mathrm{AnkleRoll}}$ indicates the control input created by the transient balance controller.

Figure 9 shows the control structure of the transient balance controller in the frontal plane. The role of the transient balance controller is recovering the inclination rather than the running trajectory command with the ankle roll joint in the frontal plane.

Similar to the system in a PD feedback controller, the angle and angular velocity of the stance leg are used to calculate the control input. Since the rate gyro measures only angular velocity, the angle is estimated by the integration of the rate gyro. The

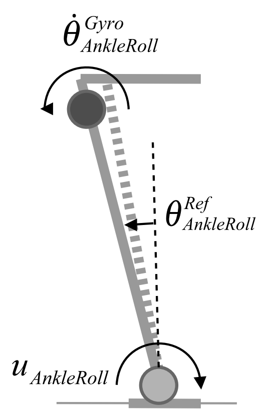

Figure 8. Simple model in the frontal plane.

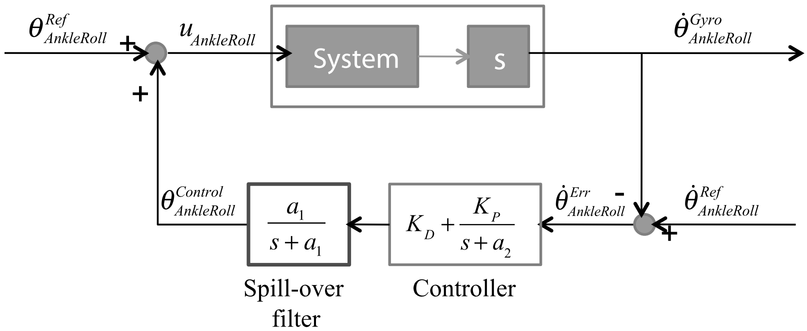

Figure 9. Block diagram of transient balance control in the frontal plane.

real angle and the estimated angle are different because of the drift of the rate gyro signal. Therefore, the drift of the rate gyro is eliminated by the high-pass filter and the integrator. Also, a spill-over filter is used to prevent unpredicted responses caused by differences between the real humanoid robot and the simple model.

The control law is:

$$\begin{aligned} u_{\mathrm{AnkleRoll}} &= \theta^{\mathrm{Ref}}_{\mathrm{AnkleRoll}} + \theta^{\mathrm{Control}}_{\mathrm{AnkleRoll}} \\ &= \theta^{\mathrm{Ref}}_{\mathrm{AnkleRoll}} + \frac{a_1}{s+a_1}\left(\frac{K_{\mathrm{P}}}{s+a_2} + K_{\mathrm{D}}\right)\left(\dot{\theta}^{\mathrm{Ref}}_{\mathrm{AnkleRoll}} - \dot{\theta}^{\mathrm{Gyro}}_{\mathrm{AnkleRoll}}\right). \end{aligned} \quad (13)$$

The structure of the transient balance controller in Fig. 9 is somewhat similar to that of the posture balance controller in Fig. 5, but the physical action of the controller is different. When the humanoid robot runs forward, it moves in the same direction regardless of the stance foot in the sagittal plane. Thus, the performance in the steady state is significant. However, since the direction of the motion in the frontal plane is changed every step, the performance in the transient state is more significant to produce balance. Therefore, on the basis of experimental experience, we use a negative feedback control in the transient balance controller. That is, the values of K_{P} and K_{D} applied to HUBO2 are positive. In the experiment, we decided that K_{P} is 0.3, K_{D} is 0.03, a_1 is 0.3 and a_2 is 0.6.

3.3. Swing Ankle Pitch Compensator in the Sagittal Plane

When the humanoid robot runs forward, it can be inclined forward or backward due to environmental factors. When it is inclined forward, the toe of the swing foot is able to touch the ground and this produces unstable running. Therefore, the toe of the swing foot is lifted up as shown in Fig. 10, according to the upper body's inclination. The inclination of the upper body is measured by the IMU sensor.

The control law is:

$$u_{\mathrm{Swing}} = \theta^{\mathrm{Ref}}_{\mathrm{Swing}} + \theta^{\mathrm{Control}}_{\mathrm{Swing}} = \theta^{\mathrm{Ref}}_{\mathrm{Swing}} + (K_{\mathrm{P}} + sK_{\mathrm{D}})\left(\theta^{\mathrm{Ref}}_{\mathrm{Swing}} - \theta^{\mathrm{IMU}}_{\mathrm{Swing}}\right), \quad (14)$$

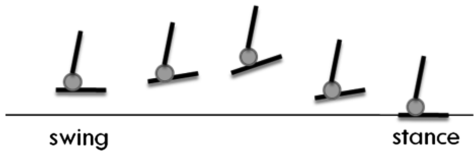

Figure 10. Motion of the swing foot.

where u_{Swing} is the input of the ankle pitch joint of the swing foot, $\theta_{\mathrm{Swing}}^{\mathrm{Ref}}$ is the desired trajectory of the ankle pitch joint of the swing foot and $\theta_{\mathrm{Swing}}^{\mathrm{IMU}}$ is the estimated angle of the ankle pitch joint of the swing foot based on the IMU sensor.

4. Experiments

The proposed controllers were applied to the humanoid robot HUBO2. Figure 11 shows the experimental results according to the existence of the posture balance controller in the sagittal plane. At this time, the transient balance controller and the swing ankle pitch compensator are working. The solid line denotes the error between the desired angle and the real angle measured by the IMU sensor of the upper body when the robot runs forward with the posture balance controller. The dashed line denotes the angle error of the upper body without the posture balance controller. When the controller is used, the error varies between $-2°$ and $2°$ and the amplitude and period are regular, as shown in Fig. 11. That is, the running is stable with the posture balance controller. On the other hand, when the controller is not used, the error is larger than the error of the controlled system, and the amplitude and period are irregular. To show the experimental results in detail, the phase portraits are plotted in Fig. 12: the left side is the phase portrait when the posture balance controller is activated and the right side is the phase portrait without activation of the controller. When the controller is used, the regular cycle is centered near the origin. On the other hand, when the controller is not used, the cycle is large and irregular. Therefore, we can see that the posture balance controller makes the robot run more stably.

Also, Figs 13 and 14 show the experimental results according to the existence of the transient balance controller in the frontal plane. The experiment was performed while the robot hopped in place, since the motion in the frontal plane is not closely related to the forward speed, unlike the motion in the sagittal plane. Even though the experiment only shows the case of hopping in place, this controller will still be effective when the robot runs at various speeds. During this experiment, the posture balance controller is always operating to reduce instability in the sagittal plane. In Figs 13 and 14, the solid line is the error between the desired upper body angle and the measured upper body angle in the frontal plane, and the dashed line is the heavily low-pass filtered error, which means the center of oscillation of the error. When the controller is used (Fig. 13), the error is between $-5°$ and $6°$, and the amplitude and period of oscillation are regular. In addition, the center of the oscillating signal,

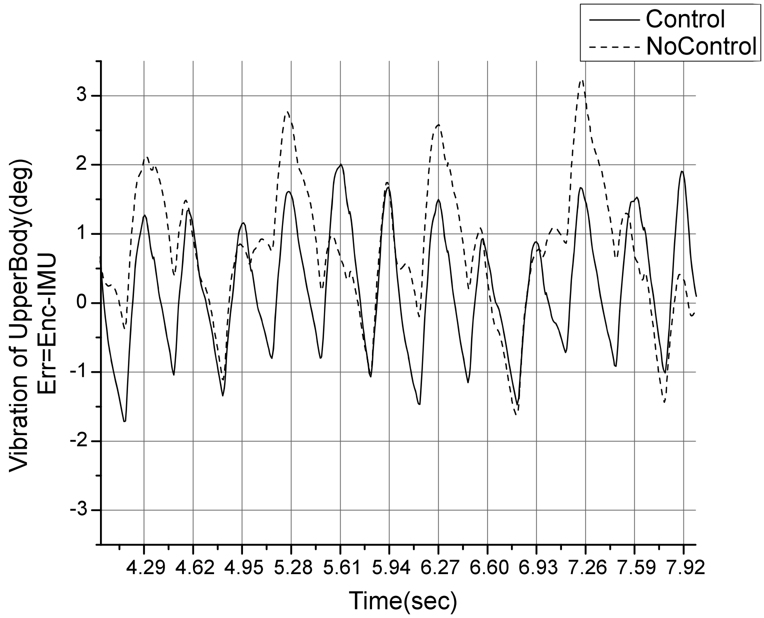

Figure 11. Experimental results of the posture balance control in the sagittal plane, speed: 2.52 km/h.

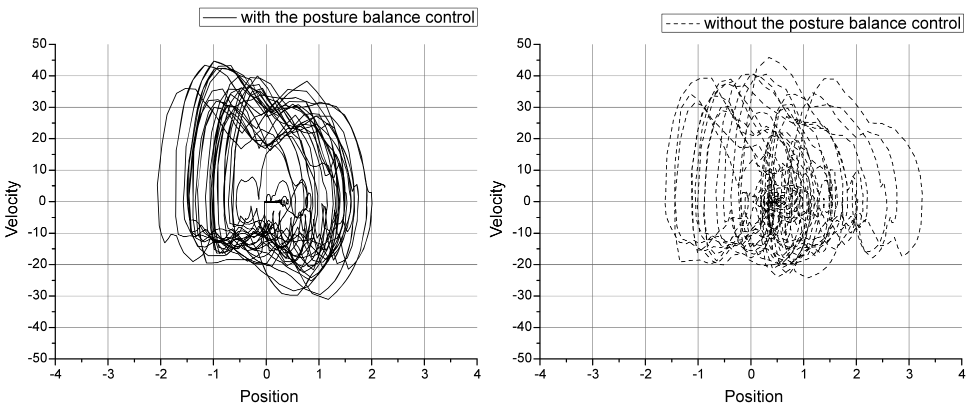

Figure 12. Phase portrait of the posture balance control in the sagittal plane, speed: 2.52 km/h.

the dashed line, is close to the x-axis, just like a straight line. That is, even though the robot vibrates in detail, the macro movement maintains a zero position. On the other hand, when the controller is not used (Fig. 14), the error is between $-8°$ and $6°$, and the amplitude and period of oscillation are more irregular. Also, the center of oscillation drifts. The phase portrait is also shown in Fig. 15: the left part shows the controlled signal and the right part shows the uncontrolled signal. The controlled signal makes a regular cycle, whereas the uncontrolled signal shows an

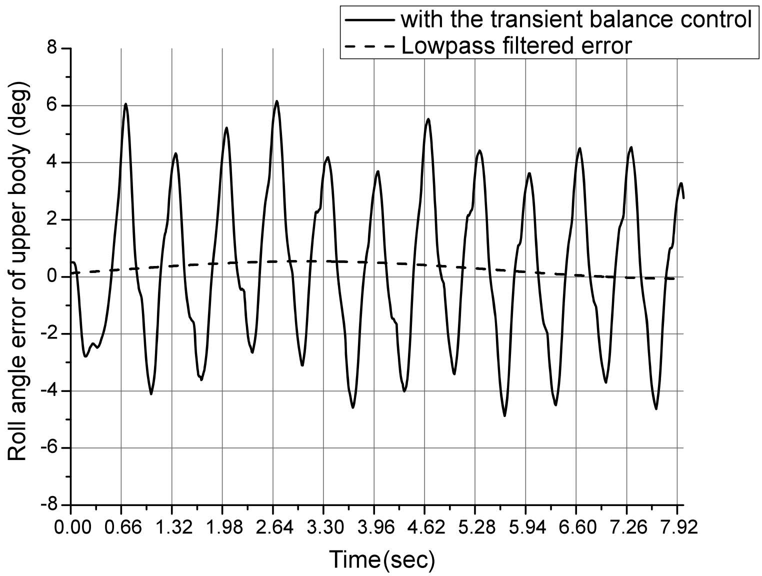

Figure 13. Experimental results with the transient balance control in the frontal plane, speed: 2.52 km/h.

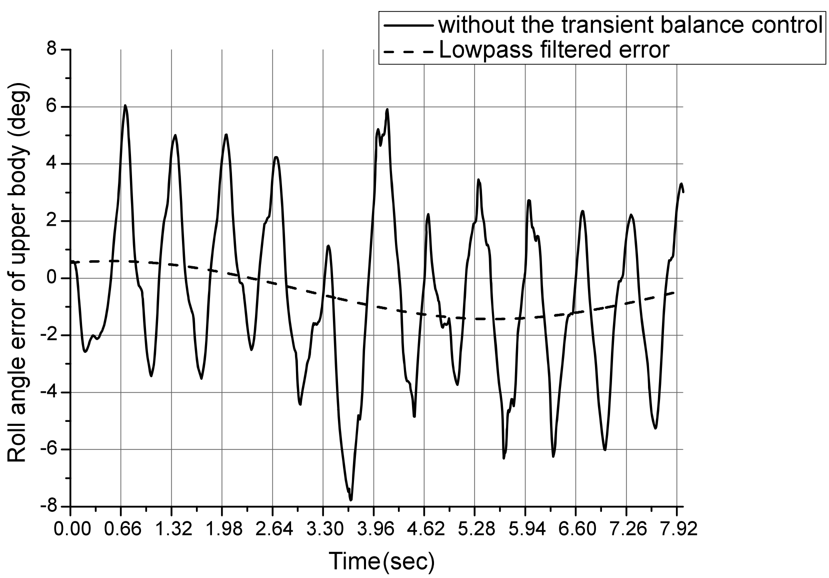

Figure 14. Experimental results without the transient balance control in the frontal plane, speed: 2.52 km/h.

irregular and large shaken cycle. Therefore, the transient balance controller makes the robot run more stably in the frontal plane.

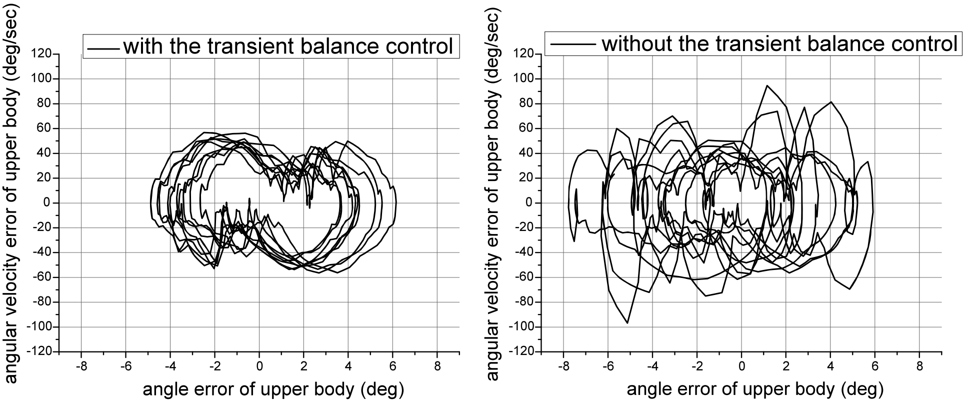

Figure 15. Phase portrait of the transient balance control in the frontal plane, speed: 2.52 km/h.

Figure 16. Photo sequence of the running experiment of HUBO2.

Finally, a running experiment was performed to verify the performance of the proposed three online controllers. With the proposed controllers, stable running was successfully achieved. Figure 16 shows a series of pictures in which HUBO2 ran. A video clip of this experiment can be seen on the website, http://hubolab.kaist.ac.kr

Table 2 shows the experimental results. HUBO2 can run at a maximum speed of 3.24 km/h. The running cycle is 0.33 s and the step length is 0.30 m. In addition, the flight time is 0.04 s and the flight length is 0.036 m.

Table 2.
Experimental result

Maximum running speed	3.24 km/h (0.9 m/s)
Running cycle	0.33 s/step
Maximum running step length	0.30 m/step
Flight time	0.04 s/step
Maximum flight length	0.036 m/step

5. Conclusion

In this paper, online controllers are proposed to achieve stable running in a humanoid robot. The controllers are composed of a posture balance controller in the sagittal plane, a transient balance controller in the frontal plane and a swing ankle pitch compensator in the sagittal plane. Controller effectiveness was verified in a running experiment. In the experiment, HUBO2 ran stably at speeds from 0 to 3.24 km/h. The contribution of the posture balance control and transient balance control on the stability was also analyzed by experiments.

In the future, the humanoid robot will be improved so that it can move faster and more stably. Also, a controller to maintain the stability of the robot according to large disturbances will be developed.

References

1. I. W. Park, J. Y. Kim, J. H. Lee and J. H. Oh, Mechanical design of humanoid robot platform KHR-3 (KAIST Humanoid Robot-3: HUBO), in: *Proc. 5th IEEE–RAS Int. Conf. on Humanoid Robots*, Tsukuba, pp. 321–326 (2005).
2. K. Kaneko, F. Kanehiro, S. Kajita, H. Hirukawa, T. Kawasaki, M. Hirata, K. Akachi and T. Isozumi, Humanoid robot HRP-2, in: *Proc. Int. Conf. on Robotics and Automation*, New Orleans, LA, pp. 1083–1090 (2004).
3. T. Takenaka, T. Matsumoto and T. Yoshiike, Real time motion generation and control for biped robot — 2nd report: running gait pattern generation, in: *Proc. IEEE/RAS Int. Conf. on Intelligent Robots and Systems*, St. Louis, MO, pp. 1092–1099 (2009).
4. T. Takenaka, T. Matsumoto and T. Yoshiike, Real time motion generation and control for biped robot — 4th report: integrated balance control, in: *Proc. IEEE/RAS Int. Conf. on Intelligent Robots and Systems*, St. Louis, MO, pp. 1601–1608 (2009).
5. R. Tajima, D. Honda and K. Suga, Fast running experiments involving a humanoid robot, in: *Proc. Int. Conf. on Robotics and Automation*, Kobe, pp. 1571–1576 (2009).
6. T. Ishida, Development of a small biped entertainment robot QRIO, in: *Proc. Int. Symp. on Micro-Nanomechatronics and Human Science*, Nagoya, pp. 23–28 (2004).
7. S. Kajita, T. Nagasaki, K. Kaneko, K. Yokoi and K. Tanie, A running controller of humanoid biped HRP-2LR, in: *Proc. Int. Conf. on Robotics and Automation*, Barcelona, pp. 618–624 (2005).
8. C. Chevallereau, E. R. Westervelt and J. W. Grizzle, Asymptotically stable running for a five-link, four-actuator, planar bipedal robot, *Int. J. Robotics Res.* **24**, 431–464 (2005).
9. M. H. Raibert, *Legged Robots That Balance*. MIT Press, Cambridge, MA (1986).

10. B. K. Cho and J. H. Oh, Running pattern generation of humanoid biped with a fixed point and its realization, in: *Proc. 8th IEEE–RAS Int. Conf. on Humanoid Robots*, Daejeon, pp. 299–305 (2008).

About the Authors

Baek-Kyu Cho was born in Hong-Sung, South Korea, in 1980. He received the BS, MS and PhD degrees in Mechanical Engineering from Korea Advanced Institute of Science and Technology (KAIST) in 2002, 2004 and 2009, respectively. In 2009, he was a Post-doctoral Researcher in KAIST. He was a researcher with the Department of Brain Robot Interface (BRI), the Computational Neuroscience Laboratories (CNS), Advanced Telecommunications Research Institute International (ATR), Kyoto 619-0288, Japan, and also with the National Institute of Information and Communications Technology (NiCT), Kyoto 619-0288, Japan. He is now a Post-doctoral Researcher in the Robotics Institute of Carnegie Mellon University. His research interests include design and control of biped humanoid robot, walking and running pattern generations, and development of devices using a microprocessor.

Jung-Hoon Kim received the BS degree in Mechanical Design and Production Engineering from Yonsei University, and the MS and PhD degrees in Mechanical Engineering from KAIST, in 1997, 1999 and 2004, respectively. From 2004 to 2005, he was a Postdoctoral Researcher at the University of California, Berkeley. From 2005 to 2006, he was a Senior Engineer at the Mechatronics Center of Samsung Electronics. He is currently an Assistant Professor in the Department of Civil and Environmental Engineering, Yonsei University, Seoul, South Korea. His research interests include design and control of biped humanoid robots, wearable exoskeleton robots, robotics in construction, and infrastructure maintenance engineering. He is a Member of the KSPE, ICROS, KSCE and KICEM.

Jun-Ho Oh received the BS and MS degrees in Mechanical Engineering from Yonsei University, Seoul, South Korea, and the PhD degree in Mechanical Engineering from the University of California, Berkeley, in 1977, 1979 and 1985, respectively. He was a Researcher with the Korea Atomic Energy Research Institute, from 1979 to 1981. Since 1985, he has been with the Department of Mechanical Engineering, KAIST, where he is currently a Professor. He was a Visiting Research Scientist at the University of Texas, Austin, from 1996 to 1997. His research interests include humanoid robots, adaptive control, intelligent control, nonlinear control, biomechanics, sensors, actuators and applications of micro processors. He is a Member of the IEEE, KSME, KSPE and ICASE.